2025 | 311

Using multi-stage Wiebe to characterize the combustion of a marine natural gas lean-burn SI engine

Dual Fuel / Gas / Diesel

Konstantinos Kiouranakis, Delft University of Technology

Peter de Vos, Delft University of Technology
Harsh Sapra, Clemson University, South Carolina
Rinze Geertsma, Faculty of Military Sciences (FMW) - Netherlands Defence Academy (NLDA)

ABSTRACT

Marine natural gas (NG) lean-burn spark-ignition (LB-SI) engines represent a promising pathway to mitigate greenhouse gas (GHG) and other hazardous emissions such as sulphur oxide (SOx), unburnt hydrocarbons (UHC) and particulate matter (PM) in the maritime sector. Converting existing diesel engines to SI operation provides a practical and scalable solution to accelerate the adoption of cleaner fuels.

Thermodynamic modeling approaches, such as Wiebe functions, can assist engine research, as they can offer a great tool for simulating combustion and providing additional insights into the characteristics of combustion. This research develops and applies multi-stage Wiebe formulations to capture the unique two-stage combustion profile of these engines, characterized by a rapid flame propagation within the bowl region followed by slower combustion in the squish region. Experimental data from load, air excess ratio, and spark timing sweeps are used to calibrate the models. Results demonstrate that while both conventional double-Wiebe and split double-Wiebe formulations effectively simulate combustion profiles, the conventional model achieves slightly higher accuracy while having fewer calibration parameters.

This study highlights how multi-stage Wiebe models can also provide qualitative insights into combustion dynamics, such as flame propagation trends under varying operating conditions. These findings contribute to better understanding how spark timing and air excess ratio influence combustion phasing, offering practical guidance for optimizing engine performance and emissions. By combining such computationally efficient tools, alongside their qualitative analysis capabilities, this framework supports further advancement in LB-SI engine technology for sustainable maritime applications.

1 INTRODUCTION

The maritime sector faces growing pressure to reduce greenhouse gas emissions and other hazardous emissions such as SOx, UHC, and PM, and transition towards cleaner energy sources. While diesel engines have long dominated power and propulsion systems of marine vessels due to their robustness and efficiency, the need to adopt sustainable fuels like methanol and hydrogen necessitates a reconsideration of alternative engine strategies that could fully leverage their emissions reduction potential [1]. Among these, spark-ignition (SI) engines emerge as a promising option [2], particularly well-suited due to the high octane-rating of many future sustainable marine fuels.

The primary challenge for SI engine technology in marine applications has always been knocking phenomena, necessitating significantly reduced compression ratios (CRs) compared to their diesel engine counterparts, which subsequently impacts efficiency. The low-speed, high-load operating regime of marine engines, combined with their substantial size, creates unfavorable conditions for flame-propagation-based combustion technologies. To mitigate knocking, such engines require highly lean mixtures and increased turbulence levels in the combustion chamber, to promote higher flame speeds and reduce knocking tendencies in the unburned fuel-air region ahead of the flame [3].

SI engine technology is not entirely new to marine applications, having been implemented in several commercial engines, primarily through lean-burn (LB) pre-chamber turbulent jet strategies [4, 5]. Pre-chamber SI engines still hold great potential for larger marine engines due to their increased capability to run on lean mixtures and enhanced knock resistance. However, the conversion of diesel engines to SI operation with minimal modifications to the diesel chamber geometry presents a simpler and more practical solution for smaller marine engines, which also typically face spatial constraints due to their typical four-valve cylinder head designs. This conversion involves replacing the diesel injector with a spark plug and integrating a low-pressure fuel injection system into the intake path for the high octane-number fuel, such as natural gas (NG).

Therefore, the combustion chamber is not redesigned to a conventional SI chamber geometry with flat piston crown and pent-roof cylinder head but maintains the bowl-in piston and flat cylinder head. This simplistic approach of keeping the diesel geometry lies in the advantages that this geometry offers with its

inducing distinct flow regime [6]. The combination of the 'swirl-killing' effect close to TDC induced by the squish region and improved tumble flow due to the bowl-in geometry, can generate high levels of turbulence in the combustion chamber that can significantly improve flame stability and speed. This improves the lean capabilities of SI engines, increasing their CR capacity, therefore efficiency, while keeping very low emissions due to lower temperatures and higher oxygen density.

Despite the potential of this strategy to accelerate the energy transition in the maritime sector, limited understanding of the distinct combustion characteristics of converted marine SI engines hinders the ability to fully leverage their performance potential. Unlike conventional SI engines, these converted engines exhibit unique combustion behavior characterized by two or even three distinct combustion phases. Optical [7] and computation fluid dynamics (CFD) modeling studies [8] have revealed that combustion in these engines primarily occurs in two stages: an initial rapid flame propagation within the bowl and a slower, delayed flame propagation in the squish region. Understanding these combustion stages and their interaction is critical for optimizing their phasing, which could significantly enhance the performance and efficiency of these engines in marine applications.

However, there remains a scarcity of research—both experimental and numerical—focused on these unique combustion phenomena, particularly for heavy-duty engines like marine. While optical and CFD studies in single-cylinder setups have provided valuable insights, the implementation of this knowledge into fast simulation tools remains underexplored. Such tools are essential for conducting parametric studies, optimization analyses, and model-based control strategies, which are vital for further improving the performance and emissions characteristics of these engines. Addressing this gap is crucial for the development of efficient, scalable solutions for marine SI engines operating on alternative fuels.

This study aims to address these gaps by developing a thermodynamic model employing multi-stage Wiebe formulations to simulate closed in-cylinder processes of a 500 kWe converted NG-SI engine. Beyond the provision of a computationally efficient thermodynamic tool, Wiebe functions can offer additional qualitative insights into two-stage combustion phenomena observed in these engines—offering guidance for optimizing performance and emissions across varying operating conditions. This modeling

approach is coupled and developed with data from recent experimental studies conducted in the engine lab of the Netherlands Defense Academy (NLDA) in Den Helder.

2 EXPERIMENTAL APPARATUS AND OPERATING CONDITIONS

The experimental setup for this research involves an 8-cylinder, four-stroke, turbocharged marine high-speed engine with a rated power of 500 kWe at 1500 rpm. This is a natural gas spark-ignition (NG-SI) powered-engine, based on the conversion of a diesel model. To minimize the modifications required on the base diesel engine, the LB-SI strategy was selected employing a new bowl-in piston, to reduce the compression ratio of the original diesel engine, and a spark plug replacing the centrally mounted diesel injector. The experimental setup at the NLDA laboratory is illustrated in Figure 1, with detailed specification provided in Table 1.

Figure 1 The marine four-stroke NG-SI engine at the NLDA lab, in Den Helder

Building accurate and fast thermodynamic in-cylinder models requires high-quality experimental data, particularly pressure and the subsequent heat release information, to ensure model accuracy and robust prediction capabilities. To this end, experimental studies preceding this research provided detailed insights into the data acquisition system, fuel composition, and combustion analysis methodology used to generate the data for this study. These experiments employed a low-calorific value and methane-number NG fuel, due to its high content in nitrogen gas. More details related to the experimental studies and methodologies can be found in references [9–11].

Table 1 Engine specifications

Engine type	8-cylinder, 4-stroke, lean-burn
Ignition mode	Spark-ignition
Combustion chamber	Flat head and bowl-in piston
Bore x Stroke [mm]	170 x 190
Displacement [L]	34.5
Rated power [kW/rpm]	500/1500
Compression ratio	12
Intake valve opening/closing [°CA aTDC]	337/-122
Exhaust valve opening/closing [°CA aTDC]	140/377
Fuel type	Natural gas

Recent experimental work focused on analyzing the engine's combustion characteristics, performance, and emissions at a constant speed of 1500 rpm across various load points, up to 432 kWe. Additionally, parametric sweeps of spark timing and air excess ratio were performed at a constant load of 200 kWe. These operating points are employed as the calibrating dataset for this modeling study.

3 MODELING METHODOLOGY

The development and application of thermodynamic engine cycle simulations have been fundamental in engine research for decades [12]. Zero-dimensional (0D) modeling stands out as the most straightforward approach for simulating the closed in-cylinder process in internal combustion engines (ICEs). This method offers notable advantages in terms of computational efficiency and predictive capability, especially when high-quality experimental data is available for calibration and validation. This study employs this 0D thermodynamic modeling approach, coupled with experimental studies, to simulate the closed in-cylinder processes of a marine NG-SI engine. The modeling framework is developed within the environment of MATLAB and Simulink [13].

3.1 Wiebe combustion modeling

To simulate the combustion process, 0D models often rely on empirical or semi-empirical sub-models calibrated using heat release data. One of the most widely used semi-empirical combustion modeling approaches is the application of the Wiebe formula, an analytical function that can effectively represent the rate of combustion [14, 15]. By employing single or multiple Wiebe functions, the Wiebe modeling approach has demonstrated its versatility in accurately capturing a wide range of combustion profiles—from the simple flame propagation

mechanism typical of SI engines [16], to two-stage diesel combustion [17], and three-stage combustion processes observed in premixed dual-fuel engines [18]. This adaptability makes Wiebe-based models a valuable tool for simulating diverse combustion behaviors across different engine concepts.

The conventional standard Wiebe functions for mass fraction burnt and rate of fuel combustion, typically used for combustion profiles in SI engines, are expressed as, respectively:

$$X_b(\theta) = 1 - \exp\left[-a\left(\frac{\theta - \theta_{SOC}}{\Delta\theta_{CD}}\right)^{m+1}\right] \quad (1)$$

$$\frac{dX_b(\theta)}{d\theta}$$
$$= \frac{a\,m}{\Delta\theta_{CD}}\left(\frac{\theta - \theta_{SOC}}{\Delta\theta_{CD}}\right)^{m}\exp\left[-a\left(\frac{\theta - \theta_{SOC}}{\Delta\theta_{CD}}\right)^{m+1}\right] \quad (2)$$

where $X_b(\theta)$ is the mass fraction burned, θ is the crank angle, θ_{SOC} is the crank angle at the start of combustion (SOC), $\Delta\theta_{CD}$ is the combustion duration, a is the efficiency parameter, m is the shape factor.

While the standard Wiebe function can accurately represent the combustion mechanism in conventional SI engines, it lacks the capability to simulate combustion profiles in alternative ICE technologies, such as diesel and dual-fuel engines. This limitation arises when the combustion process deviates from a single-stage mechanism, as is typically observed in SI engines, where a flame propagates at a relatively constant rate through the chamber until extinguished as the flame approaches the chamber walls. A notable example is the distinct combustion behavior observed in converted SI engines, which, in contrast to conventional SI, exhibits a two-stage combustion profile. Figure 2 illustrates a typical multi-stage combustion profile found in such engines. For a more in-depth discussion on the several combustion phases, the reader can refer to the study of Kiouranakis et al. [11]. To capture multi-stage combustion mechanisms, the combination of multiple Wiebe functions can be employed, expressed as:

$$X_b(\theta) = \sum_{i}^{n} b_i\left(1 - \exp\left[-a\left(\frac{\theta - \theta_{SOC}}{\Delta\theta_{CDi}}\right)^{m_i+1}\right]\right) \quad (3)$$

where b_i is the fraction of the fuel that burns during the i-th stage, and n is the number of Wiebe function used that simulate the different combustion phases. The b_i or weight factor offers

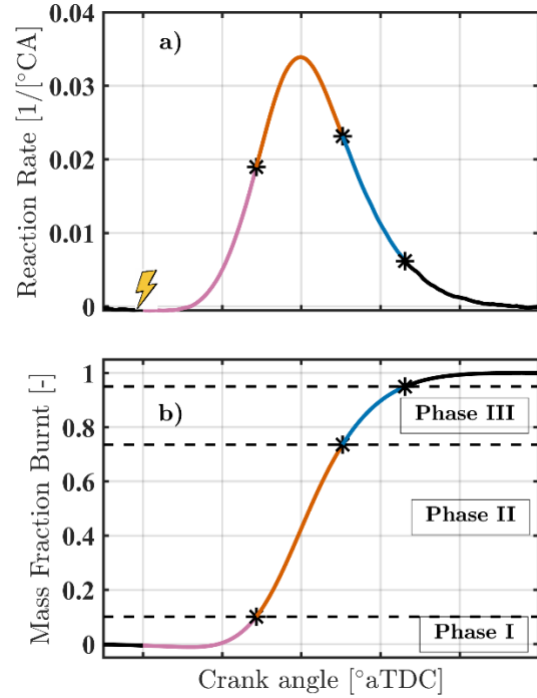a representative tool for multi-stage combustion processes.

Figure 2 The distinct combustion phases in a converted NG-SI engine, including flame development (Phase I) and bowl-in (Phase II) and squish (Phase III) combustion stage [11].

In addition to the multi-stage formulation of the Wiebe combustion model, which is employed to represent various combustion profiles observed across different engine technologies, alternative uses and adaptations of the Wiebe parameters have resulted in diverse formulations and approaches for simulating combustion profiles [16]. For instance, the conventional multi-stage Wiebe formulation, as expressed in Eq. 3, assumes similar SOC for all stages. However, distinct combustion phases in specific engine technologies can lead to abrupt peaks in heat release rate (HRR) profiles that are not adequately captured by this assumption.

To address this limitation, modified multi-Wiebe formulations have been developed that define each combustion stage that features distinct SOC, providing with a more flexible framework for such complex and non-uniform behaviors. The formulation that features distinct SOCs is expressed as:

$$X_b(\theta) = \sum_{i}^{n} H_i(\theta - \theta_{SOCi})\, b_i$$

$$\left(1 - \exp\left[-a_i\left(\frac{\theta - \theta_{SOCi}}{\Delta\theta_{CDi}}\right)^{m_i+1}\right]\right) \quad (4)$$

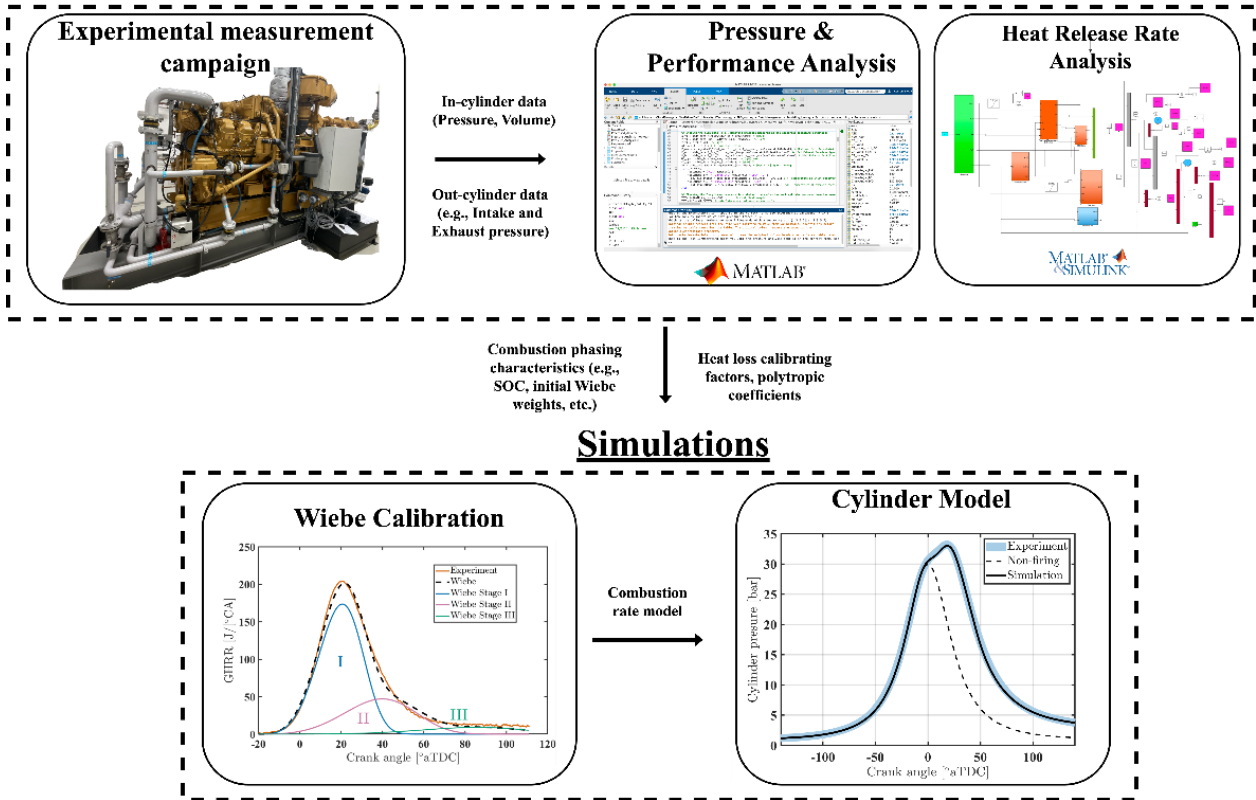# Experiments

Simulations

Figure 3 Methodology for the development and calibration of the cylindrical model based on Wiebe functions

where the $H_i(\theta, \theta_{SOC,i})$ is the Heaviside function which is introduced to ensure the estimation of the function at the corresponding combustion phase.

This study utilizes combustion data from recent experimental investigations to determine the optimal set of parameters for the Wiebe functions. Figure 3 illustrates the methodology and primary inputs used in building the model based on these experimental studies. Combustion phasing characteristics, such as the SOC and initial weight factors for multi-stage formulations, are employed as inputs for calibrating the Wiebe model parameters.

This study uses a least-square-based optimization approach to solve the resulting non-linear calibration problem:

$$G(x_i) = \; min(\textstyle\sum ||F(x_i) - y_i||^2) \qquad (5)$$

where $F(x_i)$ is the non-linear Wiebe function, y_i the experimentally estimated mass fraction burnt, and x_i is the vector containing the Wiebe calibrating parameters including the shape and duration parameters, as well as the SOC parameter for the split version of Wiebe [19].

Specifically, the MATLAB optimization toolbox function *lsqcurvefit* is utilized to determine the optimal set of Wiebe parameters. To enhance the accuracy of combustion profile representation near top dead center (TDC), primarily during the early expansion phase, an additional weighting function is applied within the crank-angle interval from -10 to 40 °CA aTDC.

The primary parameter influencing the reaction rate profile in the Wiebe model is the shape factor m_i. However, when multi-Wiebe formulation is used with adjustable combustion duration of each stage, $\Delta\theta_{CDi}$ parameter also influences the shape of the heat release profile. Figure 4 illustrates how variations in these key parameters affect the reaction rate and cumulative reaction rate profiles. While combustion efficiency a_i parameter can also influence the reaction rate profile this study assumes it relatively constant at 95% [20]. Additionally, when employing modified multi-stage Wiebe formulations, calibration includes adjusting weight factors for each combustion stage and defining SOC points for each stage. The initial parameterization for Wiebe parameters is derived from experimental analysis, and physical insight guides the selection of appropriate parameter ranges within the optimization algorithm.
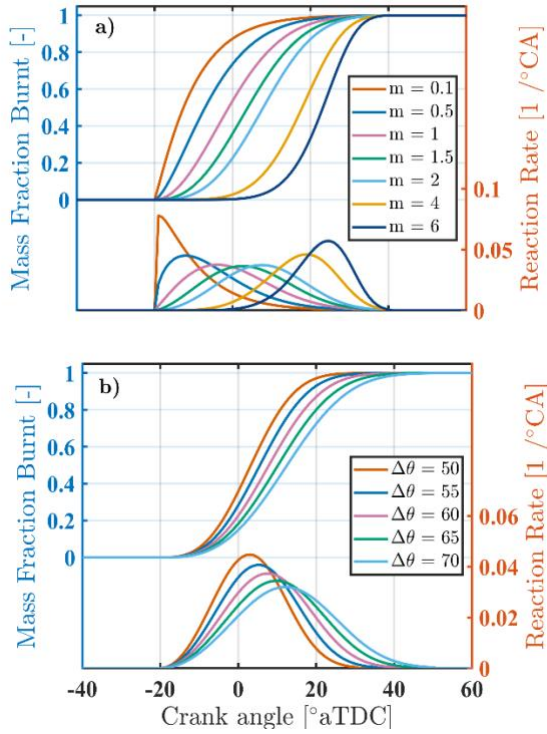
Figure 4 Sensitivity of Wiebe-based MFB and reaction rate profile to the main parameters

3.2 Closed in-cylinder process modeling

The developed combustion model is integrated into a closed 0D single-zone thermodynamic in-cylinder model. This closed cylinder model is formulated based on the solution of the ordinary differential equation derived from the first law of thermodynamics, coupled with the gas law, expressed as:

$$\frac{dT}{d\theta} = \frac{\frac{dX_b(\theta)}{d\theta} m_{\text{fuel,net}} LHV_{\text{fuel}}(\theta) n_{comb} - p \frac{dV(\theta)}{d\theta}}{m_{\text{trapped}} c_v(\theta)} \quad (5)$$

where T is the temperature, X_b is the mass fraction burnt from the Wiebe model, $m_{\text{fuel,net}}$ is the injected fuel mass, LHV_{fuel} is the lower heating value of the fuel, p is the pressure deriving from the gas law, $V(\theta)$ is the cylinder volume, m_{trapped} is the total trapped mass including residual gas mass fractions estimated through experiments, c_V is the mixture's specific heat at constant volume as derived from power series depending on both temperature and mixture's composition.

Note that the net fuel mass $m_{\text{fuel,net}}$ is utilized because the methodology is based on the apparent heat release data. To determine this net fuel mass, an estimation of the heat transfer needs to be performed to convert the measured apparent into a gross heat release, thereby connecting the experimentally measured trapped fuel mass to its net value via a heat transfer model. The heat transfer model of Woschni is used using the convective heat transfer coefficient h_{Woschni} [21], expressed as:

$$\begin{aligned} h_{\text{Woschni}} &= C_{\text{hl}} \frac{1}{D_b^{0.214}} \frac{p^{0.786}}{T^{0.523}} \Big(0.308\, c_m \\ &+ 0.00324\, \frac{p - p_{\text{mot}}}{p_{\text{IVC}}} \frac{V_{\text{stroke}}}{V_{\text{IVC}}} T_{IVC} \Big)^{0.786} \end{aligned} \quad (7)$$

where the calibrated C_{hl} for different operating points from the experimental studies is used. Once calibrated, the net mass fuel is estimated from equation:

$$m_{\text{fuel,net}} = \frac{aHRR_{cumulative}}{gHRR_{cumulative}} \quad (5)$$

The thermodynamic model is then employed during the combustion process, ranging from estimated from experimentally estimated start of combustion (SOC) to end of combustion (EOC). For non-combusting phases within the closed in-cylinder process—compression prior to SOC and expansion after EOC—polytropic functions are utilized. Polytropic coefficients of 1.35 and 1.26 are applied consistently across all operating points for compression and expansion.

3.3 Correlations for modeling parameters

Consequently, this study employs experimental data points obtained from load sweeps, as well as air excess ratio and spark timing sweeps at constant load, to establish correlations for various modeling parameters, such as the Wiebe shape factors. These correlations facilitate the effort to develop a condition-independent closed cylindrical model applicable across an operating map, defined in this engine by load, air excess ratio, and spark timing. The robustness and predictive capability of this model can subsequently be assessed and validated using additional experimental dataset distinct from those used in the calibration phase [22].

The residual sum of squares (RSS) is used to evaluate the accuracy of the models, expressed as:

$$RSS = \sum_i^n (\hat{\varepsilon}_i)^2 = \sum_i^n \big(f_{\text{model}}(x_{\text{exp}}, m, \dots) - y_{\text{exp}}\big)^2$$

where $\hat{\varepsilon}_i$ is the error term and f_{model} is the corresponding model used.

4 RESULTS & DISCUSSIONS

4.1 Wiebe model development

This section discusses the results from the capabilities of different Wiebe formulations to represent the combustion profiles in a converted NG-SI engine. As discussed in Section 3.1, previous studies have shown that standard single-Wiebe models cannot adequately capture the combustion profiles in this type of SI technology [20]. For instance, advanced spark timing can lead to "dual-peak" HRR profiles due to slower flame propagation within squish regions, requiring a multiple-stage Wiebe formulation [24]. In such cases, even two-stage Wiebe formulations may prove insufficient, necessitating a third stage to capture late burning phenomena.

However, this "dual-peak" phenomenon was not observed in any tested operating condition for this particular converted NG-SI engine, including the most advanced ignition timing and richest mixture cases [11]. This absence may be attributed to specific clearance volume characteristics influencing squish heights during expansion phases. Figure 5 illustrates HRR profiles corresponding to these most advanced ignition timing and richest mixture conditions tested experimentally that could induce such a "dual-peak" combustion phenomenon. Consequently, as demonstrated later in this section, employing a double-Wiebe formulation proves sufficient

This study explored three alternative Wiebe formulations for the first modeling approach:

1. Wiebe single mode, which uses the straightforward single-stage Wiebe function for the whole combustion process, expressed in Eq. 1. 2.

2. Wiebe double mode, which uses the double-stage Wiebe formulation, expressed in Eq. 3.

3. Wiebe double split mode, which uses the multi-stage Wiebe formulation, expressed in Eq. 4.

Figure 6 provides a comparison between experimental results and simulated reaction rate (left side) and cumulative fraction burnt (right side) profiles obtained using the three discussed Wiebe formulations at a nominal load point of 200 kWe. Table 2 summarizes the quantified information of these calibrated Wiebe modes. Although previous studies with similar SI concepts concluded that single-stage Wiebe functions are generally inadequate for accurately capturing NG-SI engine combustion profiles, this

study finds that a single-Wiebe formulation can approximate to some extent the reaction rate profile. However, it fails at capturing the combustion rate near its peak region,
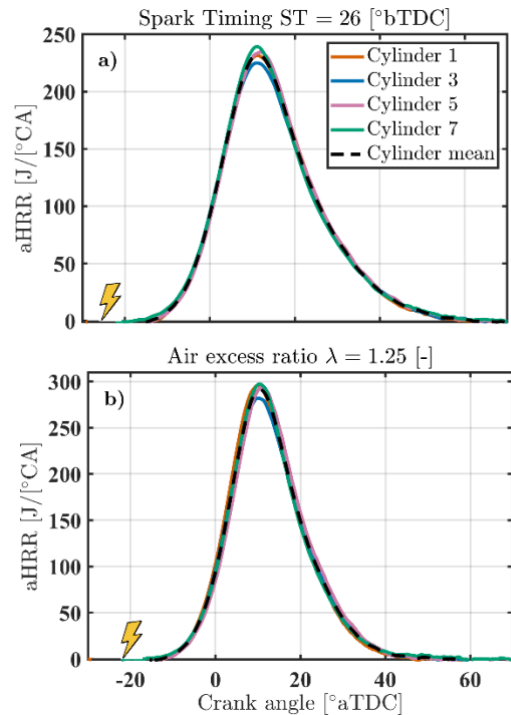

Figure 5 Experimental heat release rate profiles at the most advanced combustion phasing points tested

Regarding double-stage formulations, both conventional double-Wiebe and double-split Wiebe models effectively capture reaction rate and cumulative profiles throughout most of the combustion period. Minor discrepancies exist primarily during very early and late combustion phases; however, these phases have limited influence on critical thermodynamic properties such as in-cylinder pressure predictions. All models share an identical SOC, derived from the experimental analysis [11]. The experimental study also provides with the initial value for the SOC of the second squish combustion phase in the split version of double-Wiebe. Among the double-stage formulations evaluated, the conventional double-mode exhibits slightly higher accuracy than the double-split, achieving an RSS value of 0.15.

The calibration routine yielded different parameter values between the two double-stage models. For instance, regarding the weight factors, although both models started from identical initial values, the calibrated values diverged in opposite directions within their defined optimization ranges. The divergence is primarily attributed to differences in the SOC parameter assigned to each model. Specifically,
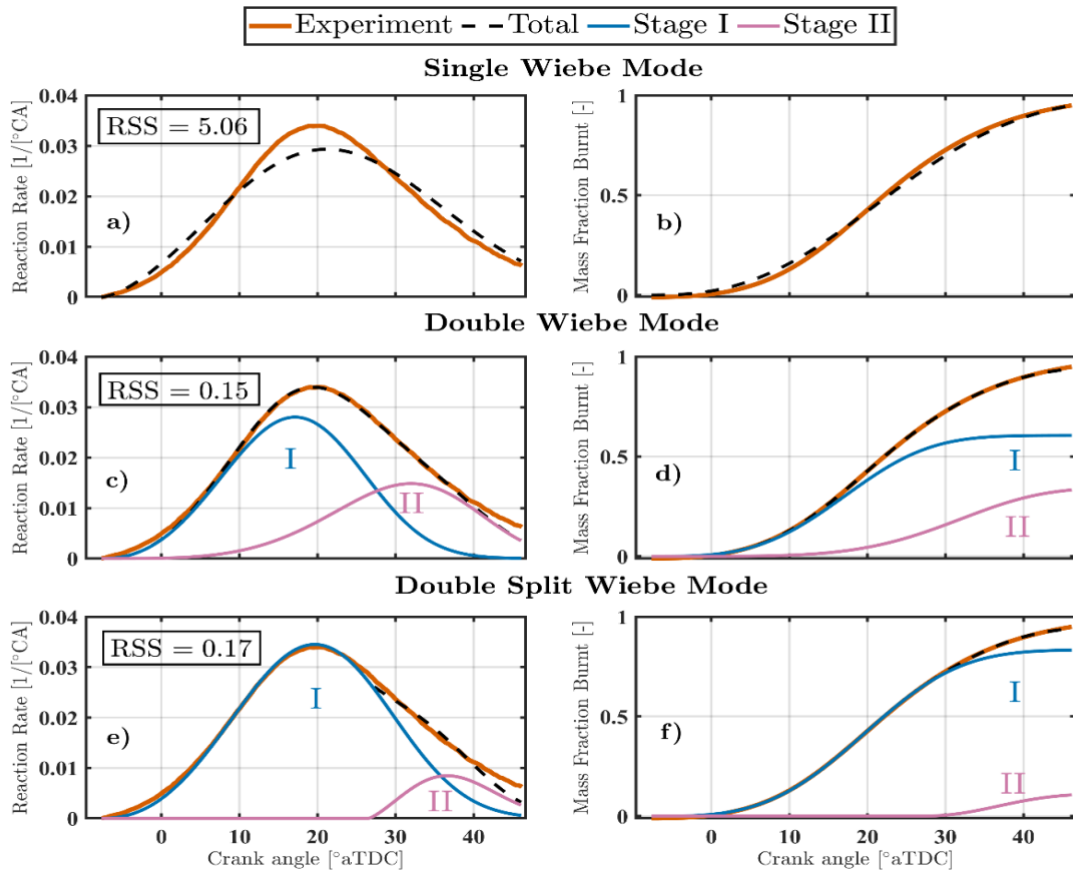
Figure 6 Experimental and simulated reaction rate and fraction burnt profiles for the different used Wiebe modes at 200 kWe load point, ST = 20°CA bTDC and λ = 1.57

in the conventional double-Wiebe formulation, the second combustion phase begins simultaneously with the first. Consequently, this formulation produces some reaction rate even at an early stage, despite representing the squish combustion phase, which is not physically expected to have started yet. This requirement leads to a reduction in the calibrated weight factor relative to its initial experimental estimate. However, this adjustment appears relatively minor as it manages to capture an expected significant overlap between the two combustion phases.

In contrast, for the split double-Wiebe formulation—where the second combustion phase initiates distinctly later—the optimization algorithm significantly reduced its weight factor magnitude to maintain a relatively smooth transition at the onset of this phase. Despite this effort, a slight abruptness in the heat release profile emerges at this transition point, an artifact not observed in the experimental heat release data. Clearly, these calibrating differences

among the weight factors influence all other parameters.

Table 2 Wiebe calibrated parameters at 200 kWe load point, ST = 20°CA bTDC and λ = 1.57

Wiebe-Mode	Parameters				RSS
	b	**m**	**Δθ**	**θ**	
Single	1	1.56	53.9	-7.7	5.06
Double	0.61	2.31	38.6	-7.7	0.15
	0.34	3.78	52.5	-7.7	
Double split	0.83	2.27	42.9	-7.7	0.17
	0.12	1.30	20.8	20.8	

However, despite these inconsistencies, something can be told about the squish combustion phasing within the combustion chamber based on the two double-Wiebe formulations. The calibrated SOC in the split version of Wiebe aligned closely with the inflection point determined in the experimental study [11]. In the conventional double-Wiebe, this appears in the vicinity of the reaction rate peak of the second phase, i.e., around 30°CA bTDC. This timing may correspond to the flame's entry into the squish region during expansion, which assumption aligns closely with previous experimental studies that correlated heat release rate profiles with optical observations [6]. Figure 7 illustrates the combustion chamber at the initiation of combustion and the estimated point at which the flame is expected to reach the squish region according to this assumption.
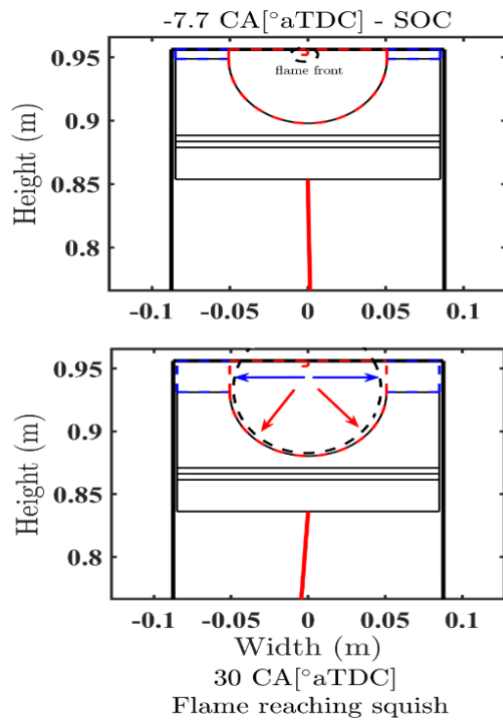

Figure 7 Approximation of a circular flame reaching the squish region

The discussion is particularly important when determining which Wiebe formulation to implement as the combustion rate model. While employing the split version and its associated second-phase SOC parameters may offer an intriguing insight into combustion phasing [25], its initiation point typically introduces some discontinuity in the overall heat release shape. If such abrupt heat release profiles had been experimentally observed, the split formulation would indeed be more appropriate for clearly distinguishing these combustion phases.

Additionally, introducing another calibration parameter inherently increases uncertainty and sensitivity within the model. This complexity comes in addition to existing uncertainties associated with other critical parameters like the weight factors of each stage, none of which can be independently validated through available experimental data in this engine.

Figure 8 confirms this added complexity, showing that while the conventional double-Wiebe has less parameters it leads to lower RSS than the split version for the majority of the operating points used for calibration. Following the parsimony principle the simples model is more appropriate [26]. To this end, the conventional double Wiebe is chosen to be applied as the combustion rate model to the cylinder model.
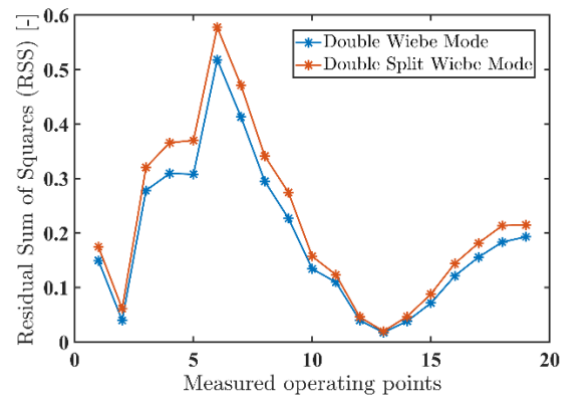

Figure 8 Residual sum of squares of the two double-stage Wiebe modes at the calibrating operating points dataset

4.2 Impact of spark timing and air excess ratio on combustion modeling phases

In addition to simulating the combustion process, the Wiebe modeling approach may offer insightful illustrations into the behavior of defined combustion stages, including their sensitivity to operating parameters. This section discusses the development of the double-Wiebe model on the experimental calibration dataset from the sweeps of air excess ratio and spark timing.

Figure 9 illustrates the reaction rates of distinct stages I and II, as modeled by the double-Wiebe formulation, across different dilution levels, covering air excess ratios λ from 1.25 to 1.77. Richer mixtures lead to a more advanced and pronounced reaction rate profile for Stage I, which represents combustion occuring primarily within the bowl region. The weight factors consistently increase for Stage I and decrease for Stage II as the mixture becomes richer. This trend aligns with the expected physical behavior of this engine configuration. Referring to the combustion chamber depicted in Figure 7, it

becomes evident that the squish-to-bowl volume ratio increases during the expansion stroke. This adds to the fact that as combustion further extends into the expansion phase, pressures from combustion will push more unburned mixture towards the periphery of the combustion chamber and subsequently the squish region [6]. Consequently, as combustion advances closer to TDC, a larger proportion is expected to combust within the bowl region rather than the squish region.
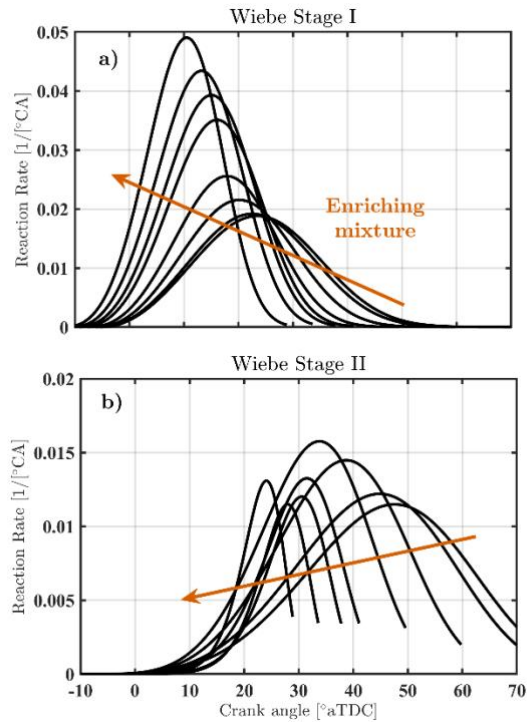

Figure 9 Reaction rate profile of the Wiebe combustion Stage I and II during the dilution sweep

As discussed in methodology and section 3.1, the shape factor m and duration factor $\Delta\theta$ are the main parameters adjusted to shape the reaction rate profile during calibration. For both stages, m actually increased with richer mixtures. Referring to Figure 4, this increase in m alone would translate into a delayed combustion phasing. However, the simultaneous decrease in $\Delta\theta$ resulted in an overall advanced and narrower reaction rate profile for richer mixtures. Therefore, when employing these Wiebe staging formulations, it is recommended to utilize both shaping parameters together rather than relying solely on the shape factor to interpret combustion characteristics such as combustion phasing. Note that the residual reaction rate observed at the end of the second stage results from that calibration performed up to CA95. Consequently, its ending phase requires smoothing before it is applied in the cylinder model.

To better illustrate the effect of air excess ratio across the swept range, Figure 10 compares reaction rate profiles for the richest and leanest mixtures tested. Enriching the mixture reduces overlap between the two combustion stages, aligning with expectations given that richer mixtures combust more fuel within the bowl region. This observations is consistent with previious studies indicating that control parameters advancing combustion phasing typically reduce stage overlap [25]. Further, as leaner mixtures are employed, reaction rate profiles for both stages widen and exhibit decreasing kurtosis, clearly demonstrating the influence of higher air excess ratios on flame propagation speed.
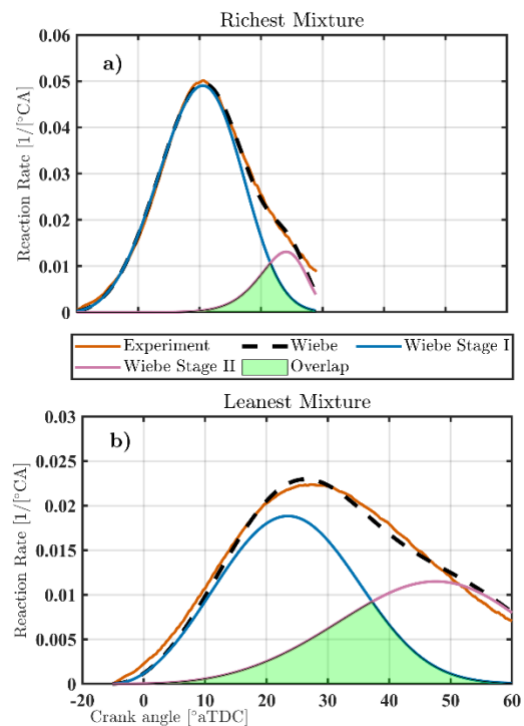

Figure 10 Overlapping of Stage I and II at the richest and leanest mixtures

Figure 11 illustrates the reaction rates of distinct stages I and II, as modeled by the double-Wiebe formulation, during a spark timing sweep ranging from 26°CA to 17°CA bTDC. Advancing spark timing exhibits a similar effect on the first combustion stage as observed with richer mixtures, although the scaling effect is smaller within the range explored in this study. However, the impact on the second combustion stage slightly diverges. While shape factor m decreases with delayed spark timing, the reduction in $\Delta\theta$ is minimal, resulting in non-consistent trend across the sweep, while some cases Stage II is even delayed while spark timing was advanced.
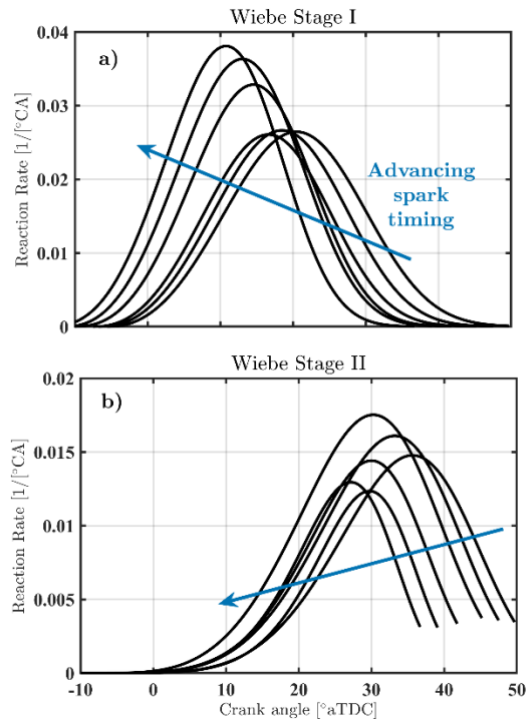
Figure 11 Reaction rate profile of the Wiebe combustion Stage I and II during the ignition timing sweep

Figure 12 Overlapping of Stage I and II at the most advanced and most retarded ignition timing

To gain a clearer insight into the ignition timing effect, Figure 12 compares reaction rate profiles for the most advanced and most retarded spark timing configurations. As expected when comparing these two extreme cases, both stages clearly advance with earlier ignition timing. Specifically, the peak reaction rate of Stage I advances from 20.5°CA aTDC to 10.6°CA aTDC, while the peak in Stage II advances from 35.8°CA aTDC to 27.4°CA aTDC. Interestingly, while peak reaction rate increases for Stage I, the reaction rate peak of Stage II actually decreases from 0.015/°CA to 0.013/°CA. This aligns well with previous experimental observations in similar engines, as well as the preceding experimental analysis conducted on this engine, highlighting the distinct sensitivity of the second combustion stage within the squish region to operating parameters such as ignition timing. To conclude, the spark timing sweep thus influences the first bowl combustion stage and second squish combustion stage differently, while this sensitivity diverge was not evident with the dilution sweep.
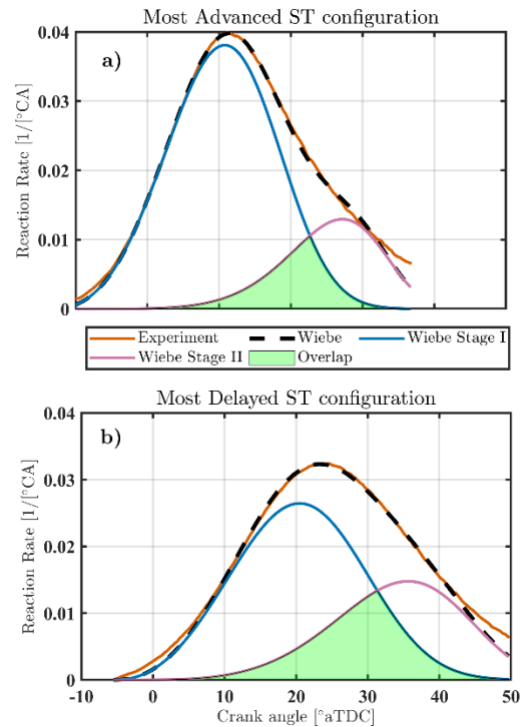
4.3   Closed in-cylinder process modeling

Following the development and evaluation of the combustion models utilizing Wiebe functions, this section discusses the application of the double-Wiebe combustion model in the thermodynamic cylinder model. The primary aim is to evaluate the cylinder's model accuracy in capturing in-cylinder processes by comparing the simulated pressure profiles with experimental measurements.

Figure 13 presents a comparison of simulated in-cylinder pressure profiles against experimental data for various load points. The thermodynamic cylinder model captured the overall pressure trends, which is consistent with the accurate reaction rate approximations achieved earlier using the Wiebe-based combustion model. The pressure profiles are similar across all load points, except for the lowest load point. This deviation is attributed to the richer mixture employed at low loads to enhance engine stability and performance under part-load conditions. Further, the use of constant polytropic coefficients for all operating points, including the operating load points illustrated in Figure 13,
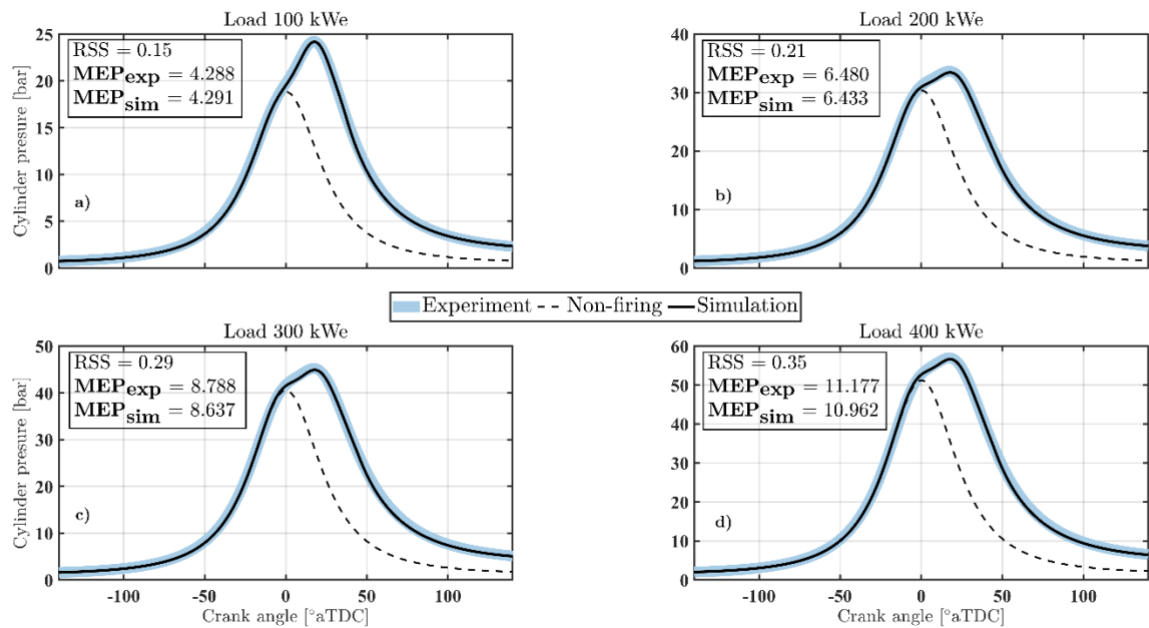
Figure 13 Simulated in-cylinder pressure against experimental results for several load points

demonstrated reliable predictions for non-combusting phases of the closed in-cylinder process.

The capability of this thermodynamic modeling approach is verified by the low RSS values and close agreement between the mean effective pressures (MEPs) of the closed cylinder process for the simulated and experimental pressure signals. The cylinder model consistently exhibits a slight underprediction of pressure, and consequently piston work, which may be attributed to minor deviations in the initial stage of the reaction rate modeled by the Wiebe functions, as seen in Figure 6c. Despite the capability of this modeling approach to capture the closed in-cylinder processes, future studies should focus on establishing correlations for various model parameters across the engine's operating map, as well as validating the model using an additional independent experimental dataset.

Figure 14 illustrates the RSS values across all operating points explored in this study, including air excess ratio and spark timing sweeps, confirming consistently low RSS at all points. Notably, the RSS remains relatively constant for operating points 2 and 6 through 19, as these correspond to the same nominal load point of 200 kWe during air excess ratio and spark timing sweeps. The increase in RSS observed at higher load points can likely be due to the greater magnitude of pressure signals at these conditions, amplifying the error between the simulated and measured values. Therefore, this trend highlights the sensitivity of RSS to variations in load magnitude when evaluating model accuracy.
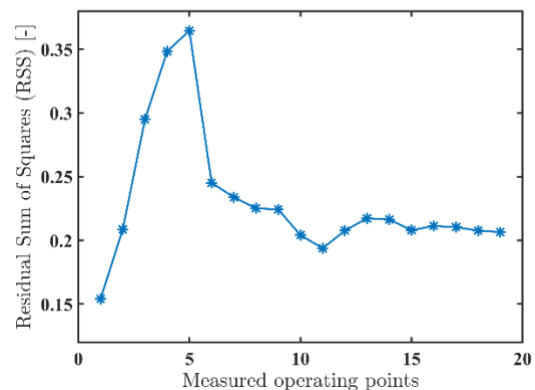

Figure 14 Residual sum of squares of the cylinder model at the calibrating operating points dataset

5   CONCLUSIONS

This study investigated the distinct combustion behavior of a 500 kWe marine natural gas (NG) lean-burn spark ignition (LB-SI) engine using a multi-stage Wiebe-based thermodynamic modeling approach. The results demonstrate that the double-Wiebe formulation is sufficient to capture the distinct combustion phases observed in these engines. The conventional double-Wiebe proved slightly more accurate than the split version, achieving lower RSS values across most operating points. This aligns with the parsimony principle, favoring simpler models for practical applications.

Beyond quantitative accuracy, this study highlights the qualitative insights provided by multi-stage Wiebe formulations. By partitioning combustion into distinct stages—such as bowl-in and squish phases—the framework enables deeper understanding of how operating parameters like spark timing and air excess ratio influence combustion phasing. For instance, advancing spark timing shifts both combustions stages earlier, while richer mixtures increase fuel burned in the bowl region, reducing overlap between stages. The multi-stage Wiebe-based thermodynamic approach can offer a fast simulation tool enabling parametric studies and model-based control strategies critical for advancing NG-SI technologies for maritime applications.

In conclusion, this study emphasizes the dual utility of multi-stage Wiebe models: as practical tools for accurate simulation and as frameworks for gaining qualitative insights into complex combustion phenomena. These contributions pave the way for further research into NG LB-SI engines and their role in supporting maritime decarbonization efforts.

6 DEFINITIONS, ACRONYMS, ABBREVIATIONS

aTDC: after Top Dead Center, **bTDC**: before Top Dead Center, **CA**: Crank Angle, **CFD**: Computational Fluid Dynamics, **CR**: Compression Ratio, **EOC**: End of Combustion, **EVO**: Exhaust Valve Open, **GHRR**: Gross Heat Release Rate, **ICE**: Internal Combustion Engine, **IVC**: Inlet Valve Close, **MEP**: Mean Effective Pressure, **NG**: Natural Gas, **IVC**: Inlet Valve Close, **RSS**: Residual Sum of Squares, **SI**: Spark Ignition; **ST**: Spark Timing;

kWe: Kilowatt-electric, **0D**: Zero-Dimensional, **rpm**: Revolutions per minute; **λ**: Air excess ratio.

7 ACKNOWLEDGMENTS

8 REFERENCES

1. Curran S, Onorati A, Payri R, et al The future of ship engines: Renewable fuels and enabling technologies for decarbonization. International Journal of Engine Research 25.1 (2024): 85-110.

2. Mahendar SK, Erlandsson A, Adlercreutz L (2018) Challenges for Spark Ignition Engines in Heavy Duty Application: a Review. SAE Technical Paper 2018-01–0907, 2018, https://doi.org/10.4271/2018-01-0907.

3. Liu J, Dumitrescu CE Flame development analysis in a diesel optical engine converted to spark ignition natural gas operation. Applied Energy 230 (2018): 1205-1217.

4. AEsoy V, Magne Einang P, Stenersen D, Hennie E, Valberg I (2011) LNG-Fuelled Engines and Fuel Systems for Medium-Speed Engines in Maritime Applications. SAE Technical Paper 2011-01-1998, 2011, https://doi.org/10.4271/2011-01-1998.

5. Humerfelt T, Johannessen E, Vaktskjold E, Skarbö L (2010) Development of The Rolls-Royce C26: 33 Marine Gas Engine Series. In: 26th CIMAC World Congress. p paper. no. 54.

6. Liu J, Dumitrescu CE Combustion partitioning inside a natural gas spark ignition engine with a bowl-in-piston geometry. Energy conversion and management 183 (2019): 73-83.

7. Dumitrescu CE, Padmanaban V, Liu J (2018) An Experimental Investigation of Early Flame Development in an Optical Spark Ignition Engine Fueled With Natural Gas. Journal of engineering for gas turbines and power 140.8 (2018): 082802.

8. Liu J, Dumitrescu CE 3D CFD simulation of a CI engine converted to SI natural gas operation using the G-equation. Fuel 232 (2018): 833-844.

9. Sapra H, Linden Y, Van Sluijs W, Godjevac M, Visser K (2019) Experimental investigations of performance variations in marine hydrogen-natural gas engines. Cimac Congress. Vol. 2019. 2019.

10. Kiouranakis KI, De Vos P, Sapra H, Geertsma R (2024) Natural Gas for Marine Lean-Burn Spark Ignition Engines: A Combustion Stability Analysis. In: ASME

2024 Internal Combustion Engine Division Fall Technical Conference. Vol. 88520. American Society of Mechanical Engineers, 2024.

11. Kiouranakis KI, De Vos P, Willems R, Sapra H, Geertsma R (2025) Heat release behavior in a marine natural gas lean-burn SI engine: Exploring the impact of bowl-in and squish phases on performance and emissions. Journal of Applied Thermal Engineering (Manuscript submitted for publication)

12. Caton JA (2015) An introduction to thermodynamic cycle simulations for internal combustion engines. Wiley, Chichester, West Sussex

13. The MathWorks Inc. (2023) MATLAB Version: 23.2.0 (R2023b).

14. Vibe II (1956) Semi-empirical expression for combustion rate in engines. Proc. Conf. Piston Engines USSR Academy of sciences, Moscow (pp. 186-191).

15. Ghojel JI (2010) Review of the development and applications of the Wiebe function: A tribute to the contribution of Ivan Wiebe to engine research. International Journal of Engine Research, 11(4), 297-312.

16. Liu J, Dumitrescu CE (2019) Single and double Wiebe function combustion model for a heavy-duty diesel engine retrofitted to natural-gas spark-ignition. Applied energy, 248, 95-103.

17. Ding Y (2011) Characterising Combustion in Diesel Engines: Using parameterised finite stage cylinder process models. Delft University of Technology

18. Xu S, Anderson D, Hoffman M, Prucka R, Filipi Z (2017) A phenomenological combustion analysis of a dual-fuel natural-gas diesel engine. Proceedings of the Institution of Mechanical Engineers, Part D: Journal of Automobile Engineering, 231(1), 66-83.

19. Coleman TF, Li Y (1996) An Interior Trust Region Approach for Nonlinear Minimization Subject to Bounds. SIAM Journal on optimization, 6(2), 418-445.

20. Rousseau S, Lemoult B, Tazerout M (1999) Combustion characterization of natural gas in a lean burn spark-ignition engine. Proceedings of the Institution of Mechanical Engineers, Part D: Journal of Automobile Engineering, 213(5), 481-489.

21. Woschni G (1967) A Universally Applicable Equation for the Instantaneous Heat Transfer Coefficient in the Internal Combustion Engine. SAE Technical Paper 670931,1967

22. B.H.Thacker, S.W.Doebling, F.M.Hemez, M.C. Anderson, J.E. Pepin, E.A. Rodriguez (2004) Concepts of Model Verification and Validation. LA-14167, 835920

23. Liu J, Dumitrescu CE (2019) Methodology to separate the two burn stages of natural-gas lean premixed-combustion inside a diesel geometry. Energy conversion and management, 195, 21-31.

24. Liu J, Bommisetty HK, Dumitrescu CE (2019) Experimental Investigation of a Heavy-Duty Compression-Ignition Engine Retrofitted to Natural Gas Spark-Ignition Operation. Journal of Energy Resources Technology, 141(11), 112207.

25. Liu J, Ulishney CJ, Dumitrescu CE (2021) Effect of Spark Timing on the Combustion Stages Seen in a Heavy-Duty Compression-Ignition Engine Retrofitted to Natural Gas Spark-Ignition Operation. SAE International Journal of Engines, 14(3), 335-344.

26. Andersson O (2012) Experiment!: Planning, Implementing and Interpreting. John Wiley & Sons